4th URSI AT-RASC, Gran Canaria, 19-24 May 2024

Analytical Model for Three Resonant Element-Based Magnetoinductive Waveguides

Connor Jenkins*(1), and Asimina Kiourti (1)
(1) ElectroScience Laboratory, Department of Electrical and Computer Engineering, The Ohio State University, Columbus, OH 43212 USA (email: jenkins.1124@osu.edu)

Abstract

Magnetoinductive waveguides (MIWs) are near-field guiding structures constructed with unit cells of electrically small resonant elements with applications ranging from wireless body area networks to wireless sensing. Previous work has derived the near-field guiding properties when the unit cell consists of either one or two resonant elements. In this work, we expand upon the MIW theory by deriving the dispersive behavior of an MIW when the unit cell consists of three resonant elements. Several simplified relationships are also presented for a variety of common geometric constraints and symmetries. The analytical model is shown to have excellent agreement with simulated results in the passband of the MIW.

1. Introduction

Magnetoinductive waveguides (MIWs) consist of a series of periodically spaced, electrically small, resonant elements. By exciting one of the elements, the current generates a magnetic field leading to coupling to neighboring elements through Faraday's Law of Induction. Through careful design of the structure, this leads to a traveling wave phenomenon [1]. In the past, MIWs have been used for a variety of applications, including communications, power transfer, and wireless sensing [2]–[4]. Recently, MIWs have found a strong place in wireless body area network applications due to their low loss, frequency independence, unobtrusiveness, and invariance to the presence of human tissue [5]–[7].

Various areas of MIW theory have been previously explored in the literature. The foundation of the work began with the analysis of MIWs constructed with a periodic unit that contained a single resonant element [1]. From there, the theory expanded to include MIWs with a periodic unit containing two resonant elements [8]. This was done by extending into a second dimension of construction (e.g., stacking two resonant loops on top of one another) or by maintaining a one-dimensional structure but alternating between different resonant elements [9]. The addition of the second resonant element in the periodic unit allowed for two passbands for the structure – through careful design this could be used to expand the passband of the structure or to give the structure two separated passbands of operation.

In this work, we expand the theory to include three resonant elements in the periodic unit of the MIW. This will potentially provide the structure with three passbands which could then be manipulated in a similar way to the two resonant element case – allowing for an even larger passband or three distinct passbands.

The rest of the paper is laid out as follows: Section 2 walks through the derivation of the dispersion relation for the three resonant element case, Section 3 analyzes the changes in the dispersion relation under various geometric simplification, Section 4 demonstrates a numerical validation of the dispersion relation, and the paper is concluded in Section 5.

2. Derivation of Dispersion Relation

The dispersion relation mathematically relates the radial frequency of operation, ω, with the complex propagation constant, $\gamma = \alpha + j\beta$, where α is the attenuation constant and β is the phase constant. To derive the dispersion relation for an MIW with three resonant elements per unit we assume that the elements are split rings loaded with capacitors without any loss of generality. We further assume that the MIW is periodic in the direction of propagation and extends to infinity in either direction. Finally, we only account for nearest neighbor interactions in the direction of propagation.

The periodic unit consists of three elements that are not necessarily identical. We denote the intrinsic impedance of each element with $Z_{0x} = R_x + j\omega L_x + \frac{1}{j\omega C_x}$ where $x = 1, 2,$ or 3 represents each respective element in the periodic unit. Additionally, each element in the periodic unit can be rotated in any orientation and shifted any distance between $[-\frac{p}{2}, \frac{p}{2}]$ where p is the geometric period of the MIW. Figure 1 shows the labeling convention for the impedance between elements in the MIW. Each impedance is of the form $Z_{nk\pm} = j\omega M_{nk\pm}$ where $M_{nk\pm}$ is the mutual inductance between the corresponding elements.

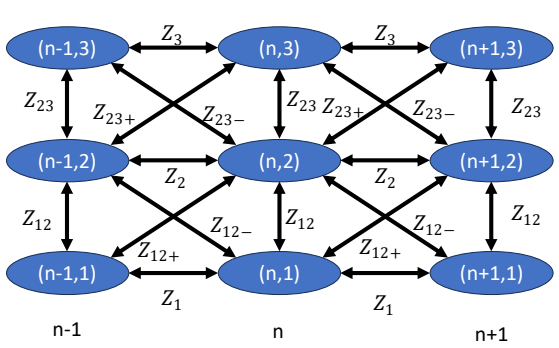

(a)

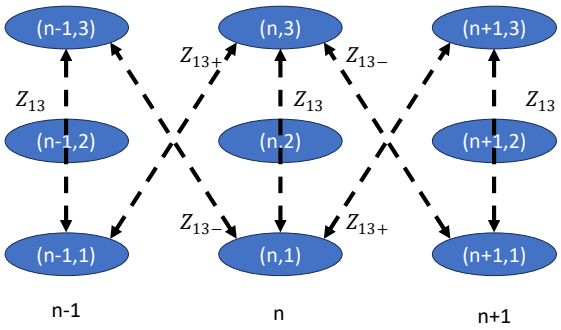

(b)

Figure 1. Diagram of impedance between neighboring MIW elements for (a) first-order interactions and (b) second-order interactions.

To derive the dispersion relation, we start by invoking Kirchoff's Voltage Law on the first element in the nth unit.

$$0 = I_{n,1}Z_{01} + I_{n-1,1}Z_1 + I_{n+1,1}Z_1 + I_{n-1,2}Z_{12-} + I_{n+1,2}Z_{12+} + I_{n,2}Z_{12} + I_{n-1,3}Z_{13-} + I_{n+1,3}Z_{13-} + I_{n,3}Z_{13} \quad (1)$$

We do the same for the second and third elements, which have similar forms as the first.

$$0 = I_{n-1,1}Z_{12+} + I_{n+1,1}Z_{12-} + I_{n,1}Z_{12} + I_{n,2}Z_{02} + I_{n-1,2}Z_2 + I_{n+1,2}Z_2 + I_{n-1,3}Z_{23-} + I_{n+1,3}Z_{23+} + I_{n,3}Z_{23} \quad (2)$$

$$0 = I_{n-1,1}Z_{13+} + I_{n+1,1}Z_{13-} + I_{n,1}Z_{13} + I_{n-1,2}Z_{23+} + I_{n+1,2}Z_{23-} + I_{n,2}Z_{23} + I_{n,3}Z_{03} + I_{n-1,3}Z_3 + I_{n+1,3}Z_3 \quad (3)$$

We now look for a wave solution to the system of equations presented. In particular, we apply $I_{n,k} = I_k \exp(j\omega t - n\gamma p)$ where I_k is the coefficient related to the element of interest. After applying this wave solution and simplifying the expressions we get:

$$0 = I_1(Z_{01} + 2Z_1\cos(j\gamma p)) + I_2(e^{j\gamma p}Z_{12-} + e^{-j\gamma p}Z_{12+} + Z_{12}) + I_3(e^{j\gamma p}Z_{13-} + e^{-j\gamma p}Z_{13+} + Z_{13}) \quad (4)$$

$$0 = I_1(e^{j\gamma p}Z_{12+} + e^{-j\gamma p}Z_{12-} + Z_{12}) + I_2(Z_{02} + 2Z_2\cos(j\gamma p)) + I_3(e^{j\gamma p}Z_{23-} + e^{-j\gamma p}Z_{23+} + Z_{23}) \quad (5)$$

$$0 = I_1(e^{j\gamma p}Z_{13+} + e^{-j\gamma p}Z_{13-} + Z_{13}) + I_2(e^{j\gamma p}Z_{23+} + e^{-j\gamma p}Z_{23-} + Z_{23}) + I_3(Z_{03} + 2Z_3 cos\ (j\gamma p)) \quad (6)$$

Up to this point, we have assumed that each element can be entirely unique. To simplify the expression significantly, we now enforce that each element is identical such that $Z_{01} = Z_{02} = Z_{03} = Z$. This allows us to solve the system of equations by algebraically eliminating the current coefficients leading to the final dispersion relation where $a_i = Z + 2Z_1\cos(j\gamma p)$ and $b_{ik+/-} = e^{j\gamma p}Z_{ik+/-} + e^{-j\gamma p}Z_{ik-/+} + Z_{ik}$.

$$a_1a_2a_3 - a_1b_{23+}b_{23-} - a_2b_{13+}b_{13-} - a_3b_{12+}b_{12-} + b_{12-}b_{13+}b_{23-} + b_{13-}b_{23+}b_{12+} = 0 \quad (7)$$

2.1. Simplifying the Dispersion Relation

While the expression for a general three-element per unit MIW is useful, often the geometry contains symmetries and uniformities that can be used to our advantage. We will look at several useful simplifications to the geometry and how the changes to the geometry impact the dispersion relation.

The first common geometric simplification is to enforce that each element is placed in the same orientation. In turn, the coupling between the n±1th unit and the nth unit is invariant to which element is examined. Mathematically, we get $Z_1 = Z_2 = Z_3$ such that $a_1 = a_2 = a_3 = a$, leading to the following simplified dispersion relation:

$$a^3 - a(b_{23+}b_{23-} + b_{13+}b_{13-} + b_{12+}b_{12-}) + b_{12-}b_{13+}b_{23-} + b_{13-}b_{23+}b_{12+} = 0 \quad (8)$$

To further simplify the expression, we can enforce that there is no shift between the elements in each unit relative to the direction of propagation (i.e., elements in each unit are aligned). With this geometry, along with the previous simplification, we now have $Z_{12+} = Z_{12-}$, $Z_{23+} = Z_{23-}$, and $Z_{13+} = Z_{13-}$. This then leads to $b_{ik} = 2Z_{ik+}cos\ (j\gamma p) + Z_{ik}$ and the further simplified dispersion relation:

$$a^3 - a(b_{23}^2 + b_{13}^2 + b_{12}^2) + b_{12}b_{13}b_{23} + b_{13}b_{23}b_{12} = 0 \quad (9)$$

By enforcing that the spacing between elements within each unit is identical in addition to the other geometric simplifications, we have $Z_{12} = Z_{23}$, $Z_{12+} = Z_{23+}$, leading to $b_{12} = b_{23}$. The dispersion relation is then further

Table I. Electrical parameters for example MIW

Parameter	Value
R	0.92 Ω
L	260.3 nH
C	56 pF
M_1	-30.3 nH
M_{12}	62.8 nH
M_{12+}	-11.3 nH

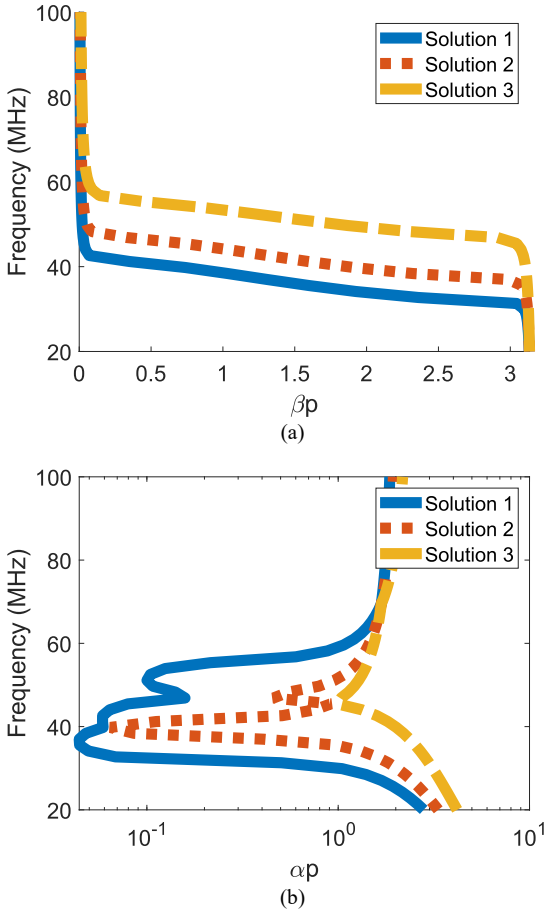

Figure 2. Dispersion diagrams for example MIW (a) phase constant and (b) attenuation constant

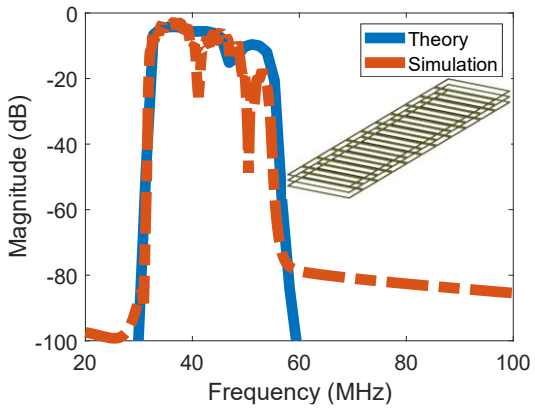

Figure 3. Comparison of theoretical and simulated results for an example MIW shown as an inset.

simplified as:

$$a^3 - a(b_{13}^2 + 2b_{12}^2) + 2b_{12}^2 b_{13} = 0 \qquad (10)$$

Finally, when the elements within each unit are spaced far enough apart such that the coupling between the first and third elements is significantly smaller than the coupling between the first and second elements, we have $Z_{13} \cong Z_{13+} \cong 0$, leading to $b_{13} \cong 0$. The dispersion relation is now in the simplest form, relying only on three impedance values (Z_1, Z_{12+} and Z_{12}) as seen in:

$$(Z + 2Z_1 \cos(j\gamma p))^3 - 2(Z + 2Z_1 \cos(j\gamma p))(2Z_{12+} \cos(j\gamma p) + Z_{12})^2 = 0 \qquad (11)$$

3. Numerical Validation

To demonstrate the utility of the dispersion relation, we examine the following geometry: Each element is constructed with 30 AWG rectangular copper loops that are 9.1 cm × 3.5 cm in size and loaded with 56 pF capacitors. The elements are all uniform, aligned, and spaced equally apart. They are placed in a planar manner such that the axes of each element in a single unit are aligned. The distance between units is 0.25 cm and the distance between the elements in each unit is 0.75 cm. With this geometry, the dispersion relation in Equation 11 is the most suitable and allows for the simplest design procedure. The equivalent electrical parameters based on this geometry are listed in Table I.

A computer algebra system was used to solve the dispersion relation for the propagation constant with the described parameters across frequency. The attenuation and phase constants vs frequency are shown in Figure 2. As expected, there are three corresponding solutions in both the phase and attenuation constants shown by the different traces. Due to the limitation of the computer algebra system, there may be some instances of discontinuities when solutions are similar in value. As shown in the attenuation constant, this design achieves a single wide passband from 31 MHz to 61 MHz. We can compare this bandwidth to the theoretical limits of a one element per unit MIW with a similar design. From the literature, we have the passband of a one element per unit MIW to be governed by:

$$\frac{1}{\sqrt{1 - 2M_1/L}} \leq \omega\sqrt{LC} \leq \frac{1}{\sqrt{1 + 2M_1/L}} \qquad (10)$$

This leads to a theoretical maximum bandwidth of 9.95 MHz which is significantly smaller than the 30 MHz bandwidth demonstrated by our simple example.

To validate the theoretical results, the geometry described was recreated in CST Studio as an 11-unit MIW and

simulated [10]. The minimum attenuation constant was taken at each frequency point, converted to dB magnitude, and compared to the simulated $|S_{21}|$ results.

Figure 3 shows the comparison between the theoretical and simulated results along with the MIW model used in simulation. As can be seen, the analytical model was able to successfully predict the performance of a finite MIW with the same structure. In fact, the model even captures the large ripples of the attenuation constant, where each band has a slight separation and slightly decreased performance. Note that the small ripples present in the simulated results are a result of reflections that arise by truncating the MIW and are not captured by the dispersion relation because of our assumption of an infinite MIW. If further fidelity in design is required, other analytical models can be used that examine the finite nature of the MIW [11].

5. Conclusion

A derivation of the relationship between the complex propagation constant and frequency of operation for a general three resonant element-based MIW was demonstrated. The relationship was further simplified for several likely scenarios such as uniform spacing and weak coupling between elements in the same unit. The analytical model was compared to simulation and showed excellent agreement within the passband of the structure. While the model agrees strongly with the presented simulation, it is important to note that this agreement is limited to MIWs with small reflections as the analytical model cannot capture this behavior effectively due to the underlying assumptions.

This derivation has set the groundwork for the expansion of MIW theory towards implementing higher numbers of resonant elements. In the future, the dispersion relation will be further analyzed to derive expressions for relevant MIW characteristics such as bandwidth and frequency of minimum attenuation.

6. Acknowledgements

This work was supported by the National Science Foundation (NSF) under grant 20053318.

References

[1] E. Shamonina, V. A. Kalinin, K. H. Ringhofer, and L. Solymar, "Magnetoinductive waves in one, two, and three dimensions," *Journal of Applied Physics*, vol. 92, no. 10, pp. 6252–6261, Nov. 2002, doi: 10.1063/1.1510945.

[2] J. Yan, C. J. Stevens, and E. Shamonina, "A Metamaterial Position Sensor Based on Magnetoinductive Waves," *IEEE Open J. Antennas Propag.*, vol. 2, pp. 259–268, 2021, doi: 10.1109/OJAP.2021.3057135.

[3] C. J. Stevens, C. W. T. Chan, K. Stamatis, and D. J. Edwards, "Magnetic Metamaterials as 1-D Data Transfer Channels: An Application for Magneto-Inductive Waves," *IEEE Trans. Microwave Theory Techn.*, vol. 58, no. 5, pp. 1248–1256, May 2010, doi: 10.1109/TMTT.2010.2045562.

[4] C. J. Stevens, "Magnetoinductive Waves and Wireless Power Transfer," *IEEE Trans. Power Electron.*, vol. 30, no. 11, pp. 6182–6190, Nov. 2015, doi: 10.1109/TPEL.2014.2369811.

[5] V. Mishra and A. Kiourti, "Wearable Magnetoinductive Waveguide for Low-Loss Wireless Body Area Networks," *IEEE Trans. Antennas Propagat.*, vol. 69, no. 5, pp. 2864–2876, May 2021, doi: 10.1109/TAP.2020.3030987.

[6] V. Mishra and A. Kiourti, "Wearable Planar Magnetoinductive Waveguide: A Low-Loss Approach to WBANs," *IEEE Trans. Antennas Propagat.*, vol. 69, no. 11, pp. 7278–7289, Nov. 2021, doi: 10.1109/TAP.2021.3070681.

[7] C. B. Jenkins and A. Kiourti, "Wearable Dual-Layer Planar Magnetoinductive Waveguide for Wireless Body Area Networks," *IEEE Transactions on Antennas and Propagation*, vol. 71, no. 8, pp. 6893–6905, Aug. 2023, doi: 10.1109/TAP.2023.3286042.

[8] O. Sydoruk *et al.*, "Tailoring the near-field guiding properties of magnetic metamaterials with two resonant elements per unit cell," *Phys. Rev. B*, vol. 73, no. 22, p. 224406, Jun. 2006, doi: 10.1103/PhysRevB.73.224406.

[9] O. Sydoruk, O. Zhuromskyy, E. Shamonina, and L. Solymar, "Phonon-like dispersion curves of magnetoinductive waves," *Applied Physics Letters*, vol. 87, no. 7, p. 072501, Aug. 2005, doi: 10.1063/1.2011789.

[10] Dassault Systemes, "Electromagnetic Simulation Solvers | CST Studio Suite." Accessed: Sep. 07, 2023. [Online]. Available: https://www.3ds.com/products-services/simulia/products/cst-studio-suite/solvers/

[11] S. Coogle, C. Jenkins, and A. Kiourti, "A Theoretical Model for Finite-Element Magnetoinductive Waveguides," in *2024 United States National Committee of URSI National Radio Science Meeting (USNC-URSI NRSM)*, Boulder, Jan. 2024.